PERGAMON

Vision Research 40 (2000) 789–803

Vision Research

www.elsevier.com/locate/visres

Detection of chromoluminance patterns on chromoluminance pedestals II: model

Chien-Chung Chen *, John M. Foley, David H. Brainard

Department of Psychology, University of California, Santa Barbara, CA 93106, USA

Received 10 February 1999; received in revised form 28 October 1999

Abstract

A model for chromoluminance pattern detection and pedestal effects is described. This model has five stages. The stimulus is first processed by the cone array and then by color-spatial linear operators. The outputs of the linear operators may be expressed as weighted sums of cone contrasts over space. There are three opposite sign pairs of linear spatial operators in the model. Their spectral tuning at each point in space is similar to the luminance, green/red and blue/yellow mechanisms in color opponent models, but their sensitivity to cone inputs varies as a function of space. The operators in each pair are the same except that the signs of the cone inputs in one are the opposite of those in the other. A non-linear response operator follows each linear operator. It receives two inputs, one excitatory and the other divisive inhibitory. The excitatory input is the half-wave rectified output of one of the linear operators. The inhibitory input is a non-linear sum of all linear operator outputs. The non-linear response operator raises the excitatory input to a power, and divides it by the inhibitory input plus a constant to produce the response. The detection variable is computed by combining the difference in response to target-plus-pedestal and pedestal alone across the three non-linear operators. The model accounts well for the large data set presented in the companion paper and is generally consistent with other results in the literature. The spectral sensitivities of the inferred chromoluminance pattern mechanisms are similar to those obtained with different methods. The data set is shown to be inconsistent with several other models.

Keywords: Color vision; Spatial vision; Contrast masking; Chromatic mechanism; Chromoluminance patterns

1. Introduction

Although the human visual system can detect and discriminate spatial patterns defined by modulation in luminance (De Valois & De Valois, 1988; Graham, 1989), in chromaticity (Cavanagh, 1991; Mullen & Kingdom, 1991; Regan, 1991; Sekiguchi, Williams & Brainard, 1993), or both (Poirson & Wandell, 1996), current quantitative models do not account for detection and discrimination of all three kinds of pattern.

There are models for luminance pattern vision (Legge & Foley, 1980; Wilson, McFarlane & Philips, 1983; Ross & Speed, 1991; Foley, 1994; Teo & Heeger, 1994; Watson & Solomon, 1997; Foley & Chen, 1999). These models postulate human pattern vision mechanisms with specific properties and the processes involved in pattern detection. Among the properties attributed to these mechanisms are receptive fields that are tuned to orientation and spatial frequency and that sum excitation linearly, a non-linear relation between excitation and mechanism response, and in the most recent models, a broadly tuned divisive inhibitory input (Foley, 1994; Teo & Heeger, 1994; Watson & Solomon, 1997). In most of these models detection is based on a non-linear sum of response differences across mechanisms.

There are also models of human color vision (Hurvich & Jameson, 1957; Guth, Massof & Benzschawel, 1980; Guth, 1991; De Valois & De Valois, 1993). These models generally assume three cone types whose responses are combined by post-receptoral mechanisms. They are designed to account for data on the detection, discrimination, and appearance of spots of light and do not incorporate spatial sensitivity. Thus, they do not

* Corresponding author. Present address: Department of Opthalmology, University of Britsh Columbia, 4480 Oak St., Vancouver, BC, Canada V6H 3V4. Fax: +1-604-8752683.

E-mail address: chen@ski.org (C.-C. Chen)

0042-6989/00/$ - see front matter
PII: S0042-6989(99)00228-X

apply to chromoluminance pattern vision in their current forms. They are also different from most pattern vision models in the processes that they assume to mediate detection and discrimination; most are linear and none incorporate divisive inhibition.

Recently, Poirson and Wandell (1996) presented a three-mechanism model designed to account for detection of chromoluminance patterns. This model extended models of human color vision by specifying a spatial sensitivity for each post-receptoral mechanism. It was not, however, designed to account for discrimination of chromoluminance patterns and did not incorporate the non-linear response function nor the divisive inhibition now thought to be necessary to account for discrimination of luminance patterns.

In this paper, we will describe a model of chromoluminance pattern vision, designed to account for both detection and discrimination threshold measurements of spatial patterns. The initial stages of the model closely resemble models of color vision; the later stages are an extension of recent models of pattern vision (Foley, 1994; Foley & Chen, 1999). Two of the ideas in the model (a) that cross-masking, both between luminance targets and isoluminant pedestals and between isoluminant targets and luminance pedestals, is due to cross-channel inhibition and (b) that cross-facilitation of an isoluminant target by a luminance pedestal is due to excitation of the chromatic channels by the luminance pattern, were proposed by Switkes, Bradley & De Valois (1988) on the basis of their chromoluminance masking results.

Below we provide a quantitative description of our model and fit the model to data presented in the companion paper (Chen, Foley, & Brainard, 1999, 2000). The principal results from our experiments to be accounted for are the following:

1. Any chromoluminance target will be masked by any chromoluminance pedestal provided that the contrast of the pedestal can be made high enough.
2. Any chromoluminance target will be facilitated by pedestals modulated (in one direction or the other) along most lines in cone contrast space, but for at least some targets there are directions such that pedestals modulated in these directions will not facilitate the target. Our data show that for luminance targets, pedestals in the individually isoluminant plane produce little or no facilitation, and for luminance, green/red, yellow-green/purple, and blue-green/orange targets, pedestals in the blue/yellow direction do not facilitate.
3. The form of the TvC functions varies greatly with the chromoluminance directions of target and pedestal.

We describe the quality of the fit and compare the performance of our model to other candidate models derived from ideas in the literature. We also use the parameters of our model fit to describe the properties of the mechanisms implied by the model. These properties include mechanism spectral sensitivities and the manner in which the divisive inhibition to each mechanism depends on the outputs of other mechanisms. We also discuss whether our model is consistent with other results in the literature.

2. The model

2.1. Overview

Since our focus is on the nature of the mechanisms and processes involved on chromoluminance pattern vision, we have included in our model only those mechanisms needed to account for our results, which are produced by patterns of one spatial frequency (1 c/deg), one orientation (horizontal), one phase relative to the fixation point (cosine) and one retinal position (centered on the fovea). It is clear from the literature on pattern vision that to account for detection and discrimination of patterns that differ from ours in spatial frequency, orientation, phase and position many more mechanisms will be needed (e.g. Wilson, Levi, Maffei, Rovamo & De Valois, 1990).

A schematic illustration of our model is shown in Fig. 1. This model has six mechanisms, organized as three pairs, each of which has four stages. The outputs of the mechanisms are combined into a single detection variable which determines the predicted threshold. The steps in the model computation are outlined below. A detailed description follows:

1. Linear operators: An input pattern is registered by each of the three cone arrays. The three cone contrasts at each point provide the input to six chromoluminance linear operators. Each linear operator defines the receptive field of the corresponding mechanism. The *excitation* of each linear operator is a weighted sum of cone excitations across space and time. The six linear operators (and their corresponding mechanisms) are grouped into three *opposite sign pairs*. Within each pair, the sensitivity of one member is simply the negative of the sensitivity of the other. There are two motivations for using opposite sign pairs. First, this corresponds to the physiology of simple cells in that individual cells do not respond to stimuli whose modulation is opposite in sign, but there exist other cells which do respond to these opposite signed stimuli. The underlying physiology, of course, is more complicated. Second, such paired mechanisms are needed to account for pattern discrimination when the spatial phase between target and pedestal differs (Foley & Chen, 1999).

2. Half-wave rectification: The excitation of each linear operator is half-wave rectified to produce *rectified excitation*. The output of a linear operator can be positive or negative. A neuron that behaves like a linear operator generally has a high maintained discharge rate and encodes positive and negative output by responding with higher or lower firing rate than the maintained discharge. However, it is known that neurons in striate cortex, which are essential to pattern vision, have little maintained discharge. Thus, a linear operator does not by itself provide a biologically plausible model for cortical neurons. To increase the biological plausibility of our model, we follow each linear operator by half-wave rectification. Non-negative outputs are also required by the model because outputs are raised to non-integral powers. This rectification takes the bipolar signal from each linear operator and converts it to a non-negative unipolar signal. Negative excitation is converted to 0.
3. Computation of inhibitory signal: For each mechanism, there is a *divisive inhibitory signal*. This signal is computed from the six rectified excitations by transforming each rectified excitation non-linearly and then forming a weighted sum. The non-linear transformation has a similar form across mechanisms. The weights in the sum are identical within an opposite sign pair but differ between pairs.
4. Computation of mechanism response: The *mechanism response* is computed as the rectified excitation raised to a power and divided by a divisive inhibitory input plus a constant. The two mechanisms in each pair are identical except that their cone inputs are opposite in sign.
5. Computation of detection variable: To predict threshold in a two-alternative forced-choice pattern discrimination experiment, the six mechanism responses are computed for the pedestal plus target and pedestal alone. The absolute value of this difference is taken for each mechanism. These absolute differences are then weighted and summed non-linearly to yield the *detection variable*. When target contrast is such that the value of this variable exceeds one, the target is above threshold. Threshold is then taken as the lowest target contrast where the detection variable is one.

2.2. Quantitative description

2.2.1. Stimulus description

The input to our model is the image seen by the three classes of cone photoreceptors. Each spatial location (x,

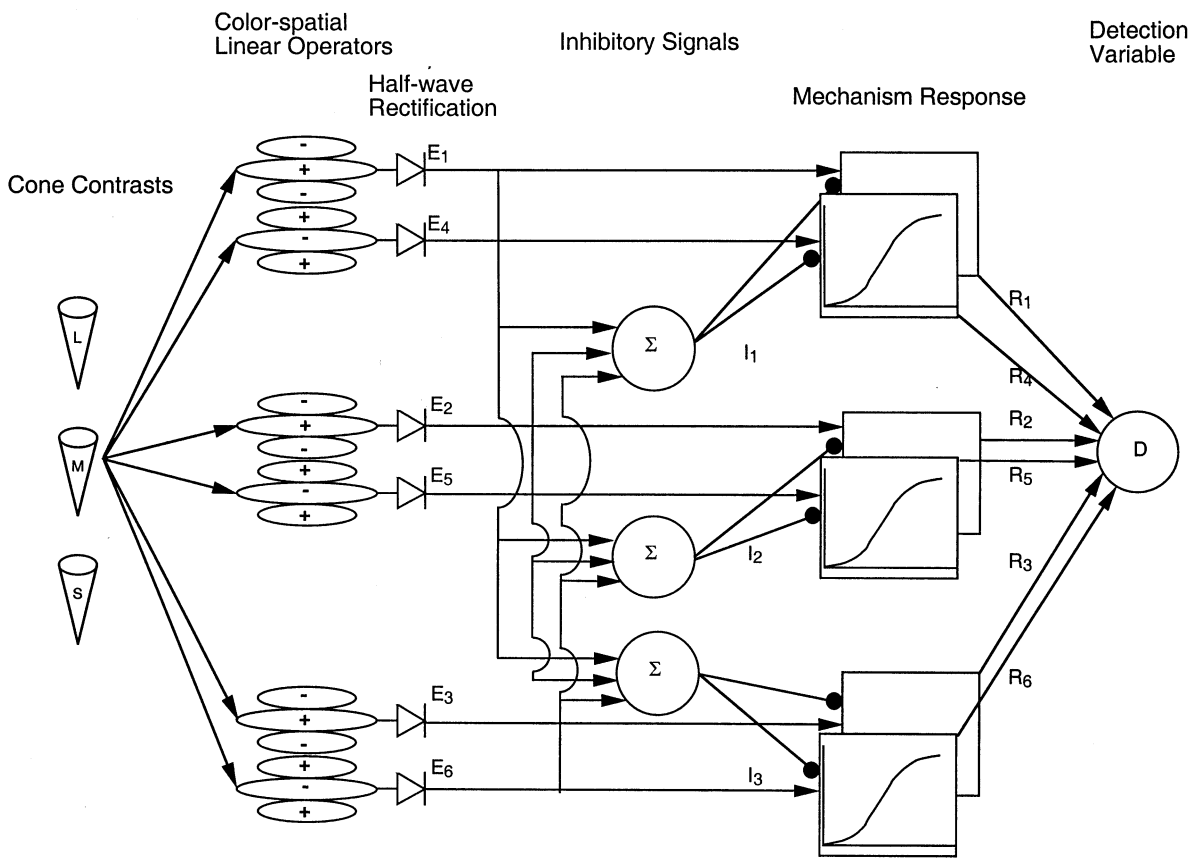

Fig. 1. A schematic diagram of the model of chromoluminance pattern detection and masking. See description in text.

Table 1
Symbols used in this article

Symbol	Meaning
$\boldsymbol{C}$	cone contrast vector of the image
C_L, C_M, C_S	L-, M-, S-cone contrasts of the image. $\boldsymbol{C} = [C_L, C_M, C_S]$
$\boldsymbol{K}(x, y)$	cone spatial excitation function
$\boldsymbol{V}(x, y)$	spatial contrast sensitivity function of a linear operator
$\boldsymbol{S_j} = [S_{Lj}\, S_{Mj}\, S_{Sj}]$	sensitivity vector of linear operator j to a chromoluminance pattern
S_{Lj}, S_{Mj}, S_{Sj}	spatial contrast sensitivity functions of linear operator j for the three cone types
E'_j	excitation of the jth linear operator
E_j	half-wave rectified excitation of jth linear operator
I_{jk}	inhibition signal from kth linear operator to jth mechanism
h_{jk}	inhibitory sensitivity to I_{jk}
I_j	total divisive inhibition to mechanism j
R_j	response of the jth mechanism
w_j	contribution of jth mechanism to detection variable
D	detection variable
.*	element by element product

y) of this image can be represented by a (column) vector-valued function $\boldsymbol{K}(x, y)$, whose three entries represent the L, M, and S cone excitation coordinates. Here we consider that class of chromoluminance patterns for which the color variation is confined to a straight line in cone excitation space. Let $P(x, y)$ define the spatial modulation of the pattern; in our experiments $P(x, y)$ specified a Gabor pattern. Let the column vector **BG** represent the excitation coordinates of the background around which the stimulus is modulated. Different stimuli are parameterized by different choices of the column vector $\boldsymbol{C}$, whose entries are the cone contrasts of the stimulus at location (0, 0). The L-cone contrast C_L at a location is defined as $\Delta L/L_{BG}$ where $\Delta L = L - L_{BG}$, L is the L-cone excitation at the location, and L_{BG} is the L-cone excitation of the background. The M-cone and S-cone contrasts, C_M and C_S, are defined similarly. The stimuli we consider (see Eq. 2 of the companion paper) have the property that $P(0, 0) = 1$, so the cone contrasts at location (0, 0) are always well-defined. A stimulus whose cone contrast vector is $\boldsymbol{C}$ can then be expressed as:

$$\boldsymbol{K}(x, y) = \mathbf{BG} + (\mathbf{BG}.^*\ \boldsymbol{C})P(x, y) \tag{1}$$

The symbol .* here means element-by-element product (Table 1). The Smith–Pokorny estimates of the cone spectral sensitivities (Smith & Pokorny, 1975; DeMarco, Pokorny & Smith, 1992) were used to compute cone excitation coordinates.

Since all of our mechanisms have the same spatial sensitivity profile (see below), it is clear that the model will be adequate only for a limited class of spatial patterns. These will be patterns to which these mechanisms are the most sensitive. Since our focus here is on chromatic sensitivity, we do not attempt to specify this class of patterns.

2.2.2. Stage 1: linear color-spatial operators

The first stage of each chromoluminance pattern mechanism consists of a receptive field-like linear operator. Each operator takes the excitations of the three cone arrays as input. Thus, the spatial sensitivity profile of a linear operator to cone excitations at position (x, y), $\boldsymbol{V}(x, y)$, can be written in row vector form as $[V_L(x, y), V_M(x, y), V_S(x, y)]$ where $V_L(x, y)$ is the sensitivity of the operator to L-cone excitation at location (x, y) and similarly for V_M and V_S. The excitation E'_j of the jth linear operator is then the inner product of the sensitivity function and the cone excitation evoked by the image:

$$E'_j = \int\int_{-\infty}^{\infty} \boldsymbol{V}_j(x, y)\boldsymbol{K}(x, y)\mathrm{d}x\mathrm{d}y \tag{2}$$

Substituting the expression for $\boldsymbol{K}(x, y)$ from Eq. (1) in Eq. (2) yields:

$$E'_j = \int\int_{-\infty}^{\infty} \boldsymbol{V}_j(x, y)\mathbf{BG}\mathrm{d}x\mathrm{d}y + \int\int_{-\infty}^{\infty} \boldsymbol{V}_j(x, y)(\mathbf{BG}.^*\boldsymbol{C})P(x, y)\mathrm{d}x\mathrm{d}y \tag{3}$$

The linear operator $\boldsymbol{V}(x, y)$ is assumed have an integral over space of zero. Thus the first term in Eq. (3) is zero and we can simplify further to write:

$$E'_j = \boldsymbol{S}_j\,\boldsymbol{C} \tag{4}$$

where:

$$\boldsymbol{S}_j = [S_{Lj}\, S_{Mj}\, S_{Sj}],$$

$$S_{Lj} = \int\int_{-\infty}^{\infty} (\boldsymbol{V}_{Lj}(x, y).^*\mathbf{BG}^T)P(x, y)\mathrm{d}x\mathrm{d}y$$

$\boldsymbol{V}_{Lj}$ is the first component of $\boldsymbol{V}_j$, and S_{Mj} and S_{Sj} are defined similarly to S_{Lj}. Thus, the output of each linear operator, E'_j, is simply a weighted sum of cone contrasts. The weights S_{Lj}, S_{Mj}, and S_{Sj} are called the contrast sensitivities of the operator j. They correspond to the excitations produced by the pattern when the cone contrasts equal 1. In general these weights depend on the spatial and temporal profiles of the stimulus, but since the class of stimuli that we are considering here all have the same spatial and temporal waveforms, these weights are constants in our model.

The simplification represented by Eq. (4) depends on the fact that the spatial and temporal profiles of our stimuli do not vary across experimental conditions and that our modulations are along a single line in color space. This was the case for our experiment (Chen et al., 2000). It also depends on the assumption that the spatial sensitivity operator, $V(x, y)$, is linear. Although

there is evidence of early non-linearities in the visual system, the assumption of linear receptive fields is a component of models of luminance pattern vision that have been shown to be consistent with a large body of data (Foley, 1994; Foley & Chen, 1997; Watson & Solomon, 1997; Boynton & Foley, 1999).

In our formulation, we do not explicitly represent time. The simplification of Eq. (4), however, seems completely reasonable for the case where the temporal profile of the stimuli is fixed across conditions, as it is for the data considered here.

In its present form, our model has three separate opposite sign linear operator pairs. The sensitivities of the mechanisms in a pair, S_L, S_M, S_S, are the same except for sign, so three sensitivities describe the sensitivity of each operator pair. These sensitivities are parameters of the model.

2.2.3. Stage 2: rectification

The output of each linear operator, E'_j, is half-wave rectified to give the excitation of the mechanism, E_j:

$$E_j = \max(0,\ E'_j) \tag{5}$$

Note that E_j is always non-negative and that for each opposite sign mechanism pair, at most one member of the pair has non-zero excitation for any given stimulus.

2.2.4. Stage 3: divisive inhibition

Divisive inhibition, or contrast normalization, has been considered as an essential feature to describe how human striate cortical neurons (Albrecht & Geisler, 1991; Heeger, 1992) or psychophysical mechanisms (Foley, 1994; Teo & Heeger, 1994; Watson & Solomon, 1997; Foley & Chen, 1999) respond to luminance patterns. Divisive inhibition is a second input to the units in addition to the input from the receptive field. This second input is derived from many pathways and acts in an approximately divisive way on the response of the unit. In our model the divisive inhibitory signal, I_j, is computed by raising the rectified excitations of each of the six mechanisms to a power and then taking a weighted sum of these values. For each mechanism, the divisive inhibition signal is formulated as:

$$I_j = \sum_{k=1,6} h_{jk}\, E_k^{q_j} \tag{6}$$

where q_j is a constant and the parameters h_{jk} are weighting factors for the divisive inhibitory input to mechanism j from the six mechanisms. This equation would allow for 36 weights, but we constrained the weights to be the same for the inputs to a pair of mechanisms and to be the same for the inputs from a pair of operators, so that there were nine free weights in our model. Further, within an opposite sign mechanism pair, we required that q_j be the same for both members.

2.2.5. Stage 4: mechanism response

The response of jth mechanism is defined as:

$$R_j = E_j^p/(I_j + Z_j) \tag{7}$$

where Z_j is an additive constant. The value of Z_j is the same for both members of an opposite sign mechanism pair.

2.2.6. Stage 5: detection variable

In the context of a two-alternative forced-choice pattern discrimination experiment, each mechanism has two responses, one is for the target-plus-pedestal and the other for pedestal alone. The prediction as to whether the target is detected or not is based on the differences in the responses to the target-plus-pedestal and to the pedestal alone. If we define ΔR_j as the jth mechanism's response to target-plus-pedestal minus its response to pedestal alone, then the detection variable D is given by:

$$D = \left(\sum_{j=1,6} w_j \left| \Delta R_j^m \right| \right)^{1/m} \tag{8}$$

where $w_j = w'_j/(w'_1 + w'_2 + w'_3)$ are weights given to response differences in mechanism j. This way of combining mechanism responses has been used successfully in many detection models. In pattern vision models mechanisms are usually not differentially weighted and $m > 2$; in that case the combination rule corresponds to probability summation (Quick, 1974). In color models m is often set equal to 2 (Wyszecki & Stiles, 1982). For members of each opposite sign mechanism pair, the weights w_j are constrained to be the same. Threshold is predicted as the lowest target contrast where D is equal to unity. Although we show a general form in Eq. (8), we fixed the exponent m equal to 2 in the model fitting procedure.

2.3. Performance of the model

We fitted our model to the data set reported in the companion paper (Chen et al., 2000). We used Powell's method (Press, Teukolsky, Vetterling & Flannery, 1986) to search for the parameters that minimize the sum of square error (SSE) of the model predictions. All data for the same observer were fitted with the same set of parameters. Although there are many parameters in the model (see Eqs. (4)–(8)), as discussed above, not all of them are free parameters. The best fit is shown as the smooth curves in the data figures of the companion paper.

The model fits the data reasonably well. The root mean square errors (RMSEs) are 1.56 dB for CCC (39 TvC functions, 335 data points), 1.52 dB for JKL (33 TvC functions, 284 data points) and 1.25 dB for JMF (nine TvC functions, 84 data points). These fit errors can be compared with the mean standard error of

measurement: 0.77 dB for CCC, 0.73 dB for JKL and 0.72 dB for JMF. Although the model does not account for all the non-random variation in the data, it does well. The number of free parameters is 29 for CCC and JKL and 17 for JMF. Except for one TvC function for a blue/yellow target on a luminance pedestal, observer JMF only observed for conditions where stimuli were confined to the isoluminant plane. Consequently, we were able to fit his data with only two opposite sign pairs, rather than three. This simplification is what reduced the number of free parameters for the model fit to his data. Table 2 lists the values of model parameters that provide the best fit the data.

Although the fit of the model to the data is reasonably good, given the large number of conditions, it does not account for all the systematic variation in the thresholds. This is evidenced by the fact that the RMSE of the model fit is about twice the mean standard error of measurement for CCC and JKL. Further, there are conditions in which the discrepancy between model and data is systematic. One example may be seen in Fig. 5b of the companion paper.

Table 2
Parameters estimated from the best fits of the model to our measurements[a]

Parameter	CCC	JKL	JMF
S_{L1}, $-S_{L4}$	110.5142	130.8416	N/A
S_{M1}, $-S_{M4}$	140.0323	64.8416	N/A
S_{S1}, $-S_{S4}$	−9.5871	−2.9356	N/A
S_{L2}, $-S_{L5}$	−118.4340	−34.9416	−98.1827
S_{M2}, $-S_{M5}$	136.1916	51.7722	175.5247
S_{S2}, $-S_{S5}$	−4.1022	1.4860	2.1567
S_{L3}, $-S_{L6}$	−50.6251	−22.8469	−35.9932
S_{M3}, $-S_{M6}$	29.3779	18.3284	23.9638
S_{S3}, $-S_{S6}$	21.1769	4.1632	20.0299
h_{11}, h_{44}, h_{14}, h_{41}	0.0709	0.3198	N/A
h_{12}, h_{45}, h_{15}, h_{42}	0.1015	0.2573	N/A
h_{13}, h_{46}, h_{16}, h_{43}	0.0538	0.0000	N/A
h_{21}, h_{54}, h_{24}, h_{51}	0.0008	0.0011	N/A
h_{22}, h_{55}, h_{25}, h_{52}	0.2361	0.0032	0.0543
h_{23}, h_{56}, h_{26}, h_{53}	0.0971	0.1614	0.1888
h_{31}, h_{64}, h_{34}, h_{61}	0.0623	0.0313	N/A
h_{32}, h_{65}, h_{35}, h_{62}	0.0064	0.0001	1.2682
h_{33}, h_{66}, h_{36}, h_{63}	0.0450	0.2675	0.2996
p_1, p_4	1.8319	2.1588	N/A
p_2, p_5	2.3389	2.6690	2.4416
p_3, p_6	2.7412	2.6241	2.6804
q_1, q_4	1.5614	1.6419	N/A
q_2, q_5	1.9135	2.8205	1.9361
q_3, q_6	2.0544	1.7336	2.2133
Z_1, Z_4	1.5703	9.0945	N/A
Z_2, Z_5	0.7022	0.1006	0.2260
Z_3, Z_6	0.2367	0.0723	1.8380
w'_1, w'_4[b]	1[b]	1[b]	N/A
w'_2, w'_5[b]	2.4355	0.0653	1[b]
w'_3, w'_6[b]	0.2159	0.6021	5.7386
m	2[b]	2[b]	2[b]

[a] Notice that the JMF data set is fitted with only two pairs of mechanisms. The subscripts 1–6 refer to the mechanisms LUM+, GR, BY, LUM−, RG, and YB.

[b] Fixed values.

2.4. The number of mechanisms

Most models of color vision have been concerned with experiments using spot stimuli and do not address the detection of chromoluminance patterns. The color opponent models of Hurvich and Jameson (1957) and Guth (Guth et al., 1980; Guth, 1991) assume that there are three post-receptoral mechanisms for chromoluminance information processing. This is consistent with our model, which posits three post-receptoral opposite sign mechanism pairs. Our generalization to opposite sign pairs is consistent with the model of De Valois and De Valois (1993).

There is recent psychophysical evidence that has been interpreted as indicating that there are mechanisms tuned to more than three directions in color space (Krauskopf, Williams, Mandler & Brown, 1986; Webster & Mollon, 1991; Li & Lennie, 1997). Would our model fit be improved by allowing more mechanisms? To answer this we fitted the same model allowing for four pairs of mechanisms. Although for CCC and JKL the number of the parameters increases from 29 to 43, there is virtually no gain in RMSE. RMSE decreases from 1.56 to 1.53 for CCC, from 1.52 to 1.51 for JKL. For JMF, the number of mechanisms doubles and the number of parameters increases from 17 to 43. However, RMSE decreases only from 1.25 to 1.19. The model with four pairs of mechanisms does not significantly improve the goodness-of-fit for any of the three observers ($F(14,42) = 0.1188$, $P > 0.9999$ for CCC; $F(14,42) = 0.039867$, $P > 0.9999$ for JKL, $F(26,42) = 0.1670$, $P > 0.9999$ for JMF). Thus, within the context of this more general version of our model, our data do not support the idea that there are more than three opposite sign mechanism pairs.

2.5. Model parameters

The excitatory sensitivities of the patterns mechanisms to the three cone contrasts correspond roughly with results in the literature. The same is true of internal mechanism parameters, p, q, and Z (Foley, 1994; Boynton & Foley, 1999; Foley & Chen, 1999). The inhibitory weights, h_{ij} and the detection variable weights, w_j, vary quite a bit from mechanism to mechanism and across the three observers. We do not attempt to explain or interpret these differences. It may be that a model with more constraints on these weights will prove to provide a satisfactory account of these data.

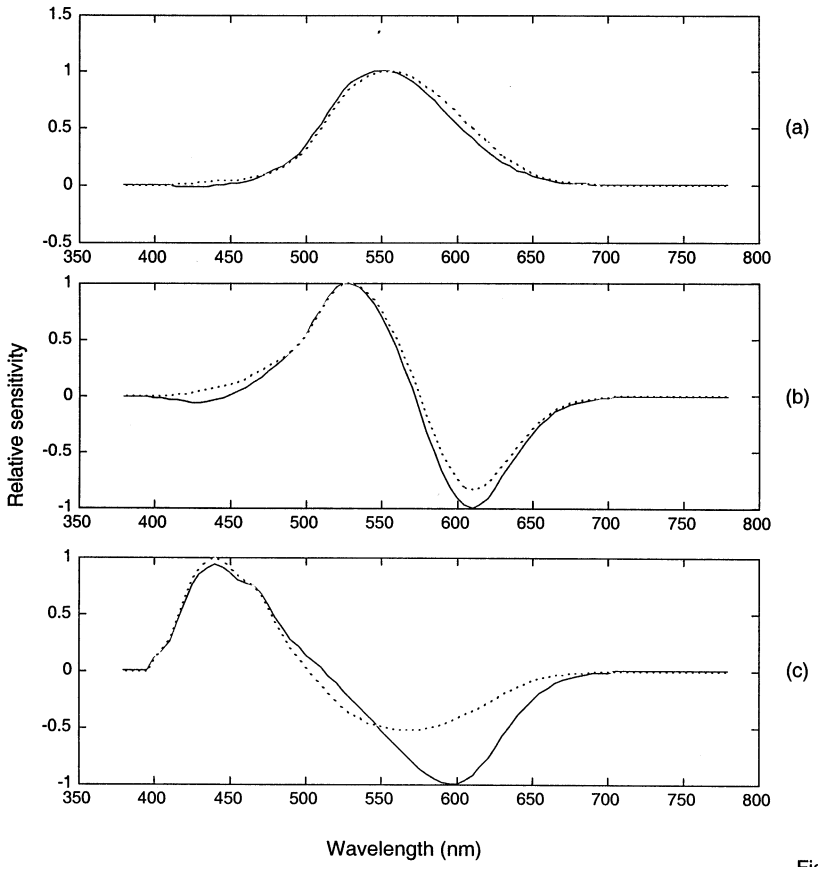

Fig. 2. Continuous curves: the spectral sensitivity functions of three of the linear operators derived from the model fit for observer CCC (top: LUM+, middle: GR, and bottom: BY). Dotted curves: upper: Vos (1978) V_λ function, middle: green/red mechanism proposed by Guth et al. (1980), lower: blue/yellow mechanism proposed by Guth et al. (1980). The other three operators have sensitivities that are the negatives of these.

2.6. Estimated spectral sensitivity of linear operators

The spectral sensitivity functions of the linear operators can be estimated from the model parameters for sensitivity to cone contrast: S_L, S_M, and S_S. Since it is customary to describe color mechanisms in terms of their sensitivity to light (spectral sensitivity) rather than their sensitivity to contrast we transformed contrast sensitivity to spectral sensitivity. Spectral sensitivity, S'_L S'_M, S'_S, is given by:

$$S'_L = S_L/L_{BG}, \quad S'_M = S_M/M_{BG}, \quad S'_S = S_S/S_{BG}, \qquad (9)$$

Fig. 2 shows the spectral sensitivity functions of the three linear operators derived from observer CCC's data. Each spectral sensitivity function is normalized by its peak value. The continuous curve in each panel shows the model estimation of one of the three of the spectral sensitivity functions, $j = 1, 2, 3$, and the dotted curves are (a) the Vos–Judd V_λ function (Vos, 1978); (b) the green/red mechanism (proposed by Guth et al. (1980) and (c) the yellow/blue mechanism proposed by Guth et al. The other three model sensitivity curves are the same except the signs are opposite. Qualitatively, our derived estimations agree roughly with the sensitivities derived from these other studies. These sensitivity functions have been referred to as luminance, red-green and blue-yellow. Our other three sensitivity functions are the same with the sign reversed. We will refer to the six sensitivity functions for $j = 1$ to 6 as LUM+, GR, BY, LUM−, RG, and YB. Figs. 3 and 4 show the same comparison for the spectral sensitivity functions derived from the data of observers JKL and JMF. JMF's data yields only two spectral sensitivity functions. Note that for all three observers L- and M-cone excitation sensitivities for the YB and BY mechanisms have opposite sign (see Table 2). This does not agree with the color opponent models proposed by Hurvich and Jameson (1957) or Guth (1991) but it does agree the proposal of De Valois and De Valois (1993).

The approximate agreement between our derived spectral sensitivities and those proposed in the literature is striking in light of the fact that nothing in our fitting procedure enforced any constraints on the shape of these functions other than that they be linear combinations of the cone sensitivities. Our model provides a

framework in which chromoluminance discrimination data for patterns of a single spatial frequency may be used to deduce properties of color vision mechanisms. Our approach here has much in common with Poirson and Wandell (1996), who analyzed detection data collected at several spatial frequencies.

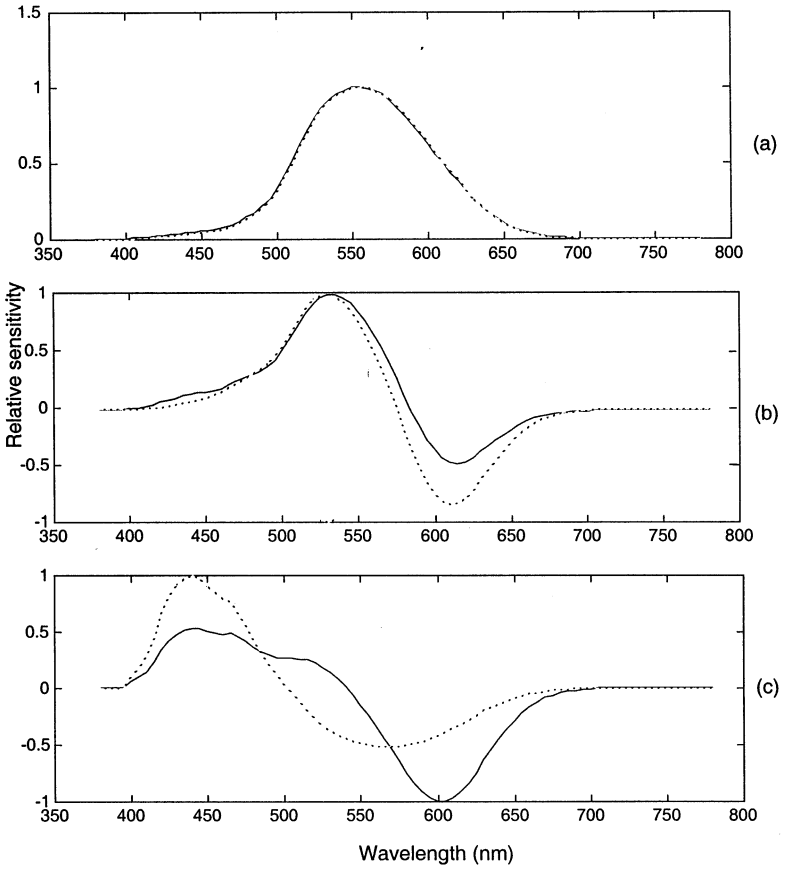

Fig. 3. Observer JKL. Same as Fig. 2.

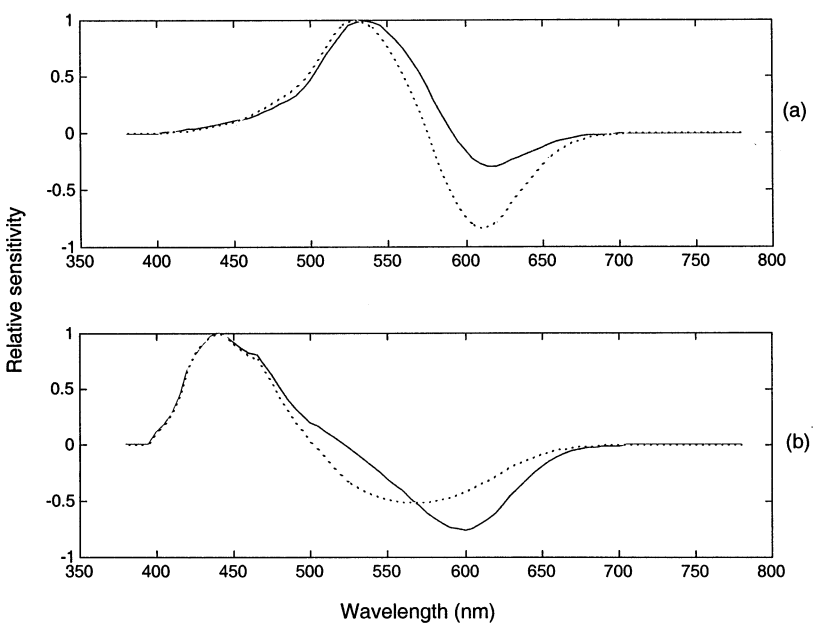

Fig. 4. Observer JMF. Same as Figs. 2 and 3 except that LUM + was not determined for this observer. (top: GR, bottom: BY).

3. Discussion

The model describes and explains the principal facts about chromoluminance pedestal effects. It predicts that a chromoluminance pedestal in any chromoluminance direction will mask a target in any direction, provided that the pedestal contrast is high enough. This is a consequence of the fact that each mechanism receives divisive inhibitory inputs from mechanisms with all three spectral sensitivity functions. It explains facilitation by an excitatory input to the detecting mechanism produced by the pedestal and the absence of facilitation by the lack of such an input, which occurs when the pedestal lies in a plane orthogonal to the direction of the mechanism. (The individually isoluminant pedestals are orthogonal to the LUM mechanism, while the luminance pedestal is not orthogonal to the GR and BY mechanisms). Two aspects of the model contribute to its account of the varying forms of the TvC functions. First, the relative strengths of excitation and divisive inhibition vary according to target and pedestal direction and contrast (e.g. Fig. 1a of the companion paper). Second, the TvC curve for a fixed pedestal direction can be mediated by the action of more than one mechanism. For example, mechanism transitions account for the complex form of the TvC functions predicted for some conditions (e.g. Figs. 4b and 6a of the companion paper).

3.1. Can a simpler model account for the data?

As noted in the introduction, we are aware of no models that directly address chromoluminance pattern detection and discrimination. Nonetheless, it is possible to extend extant models so that they make predictions for pedestal effects and to compare their performance with that of our model. Here we do this by considering models which are close to those in the literature. This is a broad class of models, but it does not include all possible models. In particular, it does not include models in which the pattern mechanisms respond to the background. As outlined below, each of these models can be obtained by changing some of the assumptions of our model or by constraining the values of some of its parameters. We show that most of these models make qualitative errors in predicting our experimental results and all of them provide poorer fits to the data. The fits produced by the various models are illustrated by showing TvC functions for the same three conditions for each model. In each case the model was fitted to the entire data set. The example conditions illustrated are those in which the target is green/red and the pedestals are green/red, blue/yellow and luminance. The fit of our model to these data is shown in Fig. 5(a). Data are shown for one observer, CCC. Data for the other observers are similar.

The two-stage color opponent model of Hurvich and Jameson (1957) is a linear response model in the sense that the outputs of the linear operators feed directly into a detection variable without intervening non-linearities. Thus, the mechanism responses are linearly related to intensity and therefore to contrast. Line element theories (Helmholtz, 1896; Le Grand, 1949; Wandell, 1982) are also linear response models in this sense, since the only non-linearity in these theories is in the rule that pools the output of multiple mechanisms.

First consider a single mechanism version of a linear response model. Such a model predicts that threshold is reached when target contrast modulates the mechanism response (either up or down) by a fixed criterion amount. Whatever the pedestal, the effect of the target will be the same linear function of target contrast. Thus a one mechanism linear response model predicts that the target threshold is independent of pedestal chromoluminance direction and pedestal contrast. Clearly, the one mechanism linear response model is qualitatively rejected by our data. Adding multiple mechanisms does not change the situation. By the same argument, the incremental response of each mechanism to the target is not affected by the presence of a pedestal and therefore the detection variable for a given target is also not affected.

To measure goodness of fit, we fitted a three mechanism pair version of a linear response model to our data. This model was like our full model except that the computation of mechanism response R_j (Eq. (7)) was replaced by the simpler expression:

$$R_j = E'_j = \mathbf{S}_j \boldsymbol{C} \tag{10}$$

where (as in Eq. (4)) $\boldsymbol{C}$ specifies the contrast of the pattern and $\boldsymbol{S}_j$ specifies the contrast sensitivity of the jth mechanism pair. Thus in our linear response model, there is no rectification, no divisive inhibition and no non-linearity except in the pooling of response differences (Eq. (8)). Here and in the other models discussed below we used the same pooling rule as for our full model (Eq. (8)). The fit of the linear response model to our data is illustrated in Fig. 5(b). As argued above, the linear response model predicts no effect of the pedestal and the predicted TvC functions are thus horizontal lines. The model fails in a similar way in other conditions. The model clearly fails to account even roughly for the measured pedestal effects. The RMSE's of this model for our entire data set are 4.54 for CCC, 2.91 for JKL and 3.59 for JMF. Although the linear model can be rejected on qualitative grounds, its RMSE's give an indication of the improvement in fit that could potentially be provided by a better model.

De Valois and De Valois (1993) extended the linear response model by adding a half-wave rectification operation to the linear operator outputs. When the

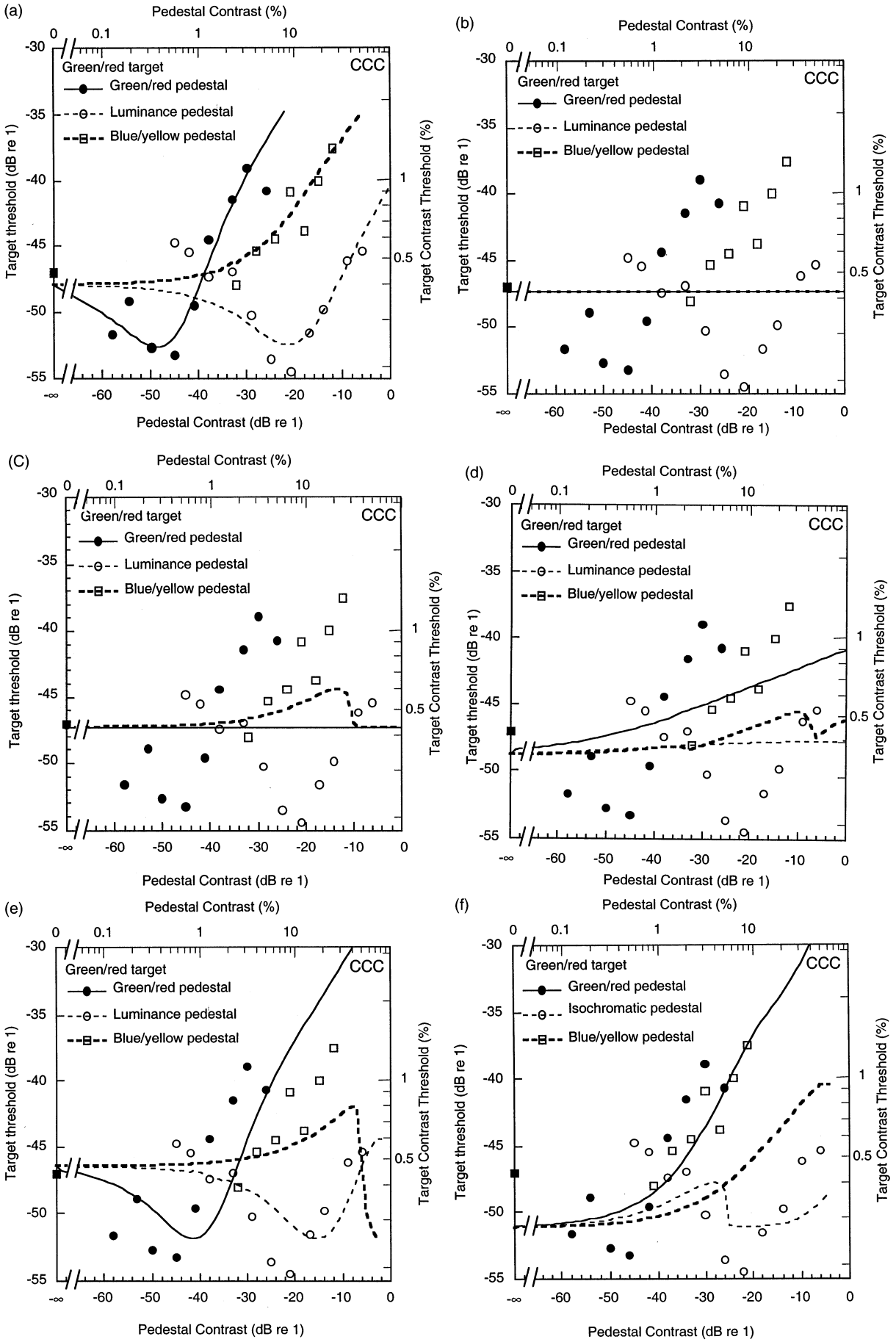
(a)
Pedestal Contrast (%)
0 0.1 1 10
Green/red target
CCC
Green/red pedestal
Luminance pedestal
Blue/yellow pedestal
Target threshold (dB re 1)
Target Contrast Threshold (%)
-30 -35 -40 -45 -50 -55
1 0.5
-∞ -60 -50 -40 -30 -20 -10 0
Pedestal Contrast (dB re 1)
(b)
Pedestal Contrast (%)
0 0.1 1 10
Green/red target
CCC
Green/red pedestal
Luminance pedestal
Blue/yellow pedestal
Target threshold (dB re 1)
Target Contrast Threshold (%)
-30 -35 -40 -45 -50 -55
1 0.5
-∞ -60 -50 -40 -30 -20 -10 0
Pedestal Contrast (dB re 1)
(C)
Pedestal Contrast (%)
0 0.1 1 10
Green/red target
CCC
Green/red pedestal
Luminance pedestal
Blue/yellow pedestal
Target threshold (dB re 1)
Target Contrast Threshold (%)
-30 -35 -40 -45 -50 -55
1 0.5
-∞ -60 -50 -40 -30 -20 -10 0
Pedestal Contrast (dB re 1)
(d)
Pedestal Contrast (%)
0 0.1 1 10
Green/red target
CCC
Green/red pedestal
Luminance pedestal
Blue/yellow pedestal
Target threshold (dB re 1)
Target Contrast Threshold (%)
-30 -35 -40 -45 -50 -55
1 0.5
-∞ -60 -50 -40 -30 -20 -10 0
Pedestal Contrast (dB re 1)
(e)
Pedestal Contrast (%)
0 0.1 1 10
Green/red target
CCC
Green/red pedestal
Luminance pedestal
Blue/yellow pedestal
Target threshold (dB re 1)
Target Contrast Threshold (%)
-30 -35 -40 -45 -50 -55
1 0.5
-∞ -60 -50 -40 -30 -20 -10 0
Pedestal Contrast (dB re 1)
(f)
Pedestal Contrast (%)
0 0.1 1 10
Green/red target
CCC
Green/red pedestal
Isochromatic pedestal
Blue/yellow pedestal
Target threshold (dB re 1)
Target Contrast Threshold (%)
-30 -35 -40 -45 -50 -55
1 0.5
-∞ -60 -50 -40 -30 -20 -10 0
Pedestal Contrast (dB re 1)

Fig. 5.

target excites one member of an opposite sign pair and the pedestal excites the other, this type of model can predict masking. However, the masking predicted by a rectified linear response model does not account quantitatively for the effects we measured. We fitted a three mechanism pair version of a linear response model with rectification to our data. The model was obtained by constraining parameters of our full model as follows: $h_{ij} = 0$, $Z_j = 1$, $p_j = 1$, $q_j = 1$. The fit is illustrated in Fig. 5(c) and the predicted TvC functions are radically different from the measured functions. The RMSE's of this model are 4.37 for CCC, 2.81 for JKL and 3.51 for JMF.

It appears that to account for facilitation and masking, an additional non-linear process must be added to the computation of the mechanism responses. Fechner (1859/1966) suggested a compressive non-linearity to explain the increase in discrimination thresholds as stimulus magnitude increases. We implemented this idea and investigated whether the resulting model could account for our data. Our implementation was a special case of our full model with constraints on some of the parameters: $h_{ij} = 0$, $Z_j = 1$, $q_j = 1$. For values of p_j less than 1, the mechanisms of this model have a compressive non-linearity and can produce masking but not facilitation. For values of p_j greater than 1, the mechanisms have an expansive non-linearity and can produce facilitation but not masking. In our fit, we allowed the p_j to vary independently for each mechanism pair, so as to allow the possibility of both masking and facilitation from the overall model. We found that to best account for our data, all three pairs of mechanisms are compressive. The fit of this model is illustrated in Fig. 5(d). The fit is again quite poor and the model does not capture the facilitation shown clearly in the data. The RMSE's of this model are 3.79 for CCC, 2.83 for JKL and 3.32 for JMF.

More generally, one can consider arbitrarily complex static non-linearities. Legge and Foley (1980) proposed a model with an S-shaped non-linearity, accelerating then decelerating as contrast increases. Wilson et al. (1983) proposed a similar model. The Legge–Foley type of model predicts both facilitation and masking. However, it also has a major limitation. Consider first a single mechanism version of this model. It predicts that the TvC function will have a particular dipper-shaped form when the pedestal produces positive excitation in the detecting mechanism and a particular monotonic increasing form when the pedestal produces negative excitation in the detecting mechanism. Other changes in the pedestal can only shift these functions laterally by a multiplicative constant (Foley, 1994). Clearly this one mechanism static non-linear model is inconsistent with our data. For a multiple mechanism model of this same type, predicted threshold is the same as that of the most sensitive mechanism (or lower if more than one mechanism makes a significant contribution to detection). This implies that when there is facilitation, its magnitude will be approximately the same. This is not consistent with our results.

We fitted a three-mechanism pair version of the Legge–Foley type model to our data. Our implementation was like our full model except that the computation of mechanism response R_j (Eq. (7)) was replaced by the expression:

$$R_j = E_j^{p_j}/(E_j^{q_j} + Z_j) \tag{11}$$

where E_j is the half-wave rectified output of the jth linear operators (as defined in Eq. (5)) and p_j, q_j, and Z_j are constants that are free to vary between mechanism pairs. The fit is illustrated in Fig. 5(e). Two of the TvC functions are horizontally shifted copies of each other. The third, for the blue/yellow pedestal, shows clearly the effect of the combination of multiple mechanisms. As the figure illustrates, the best fit of the Legge–Foley model to our data set makes dramatic prediction errors for some target-pedestal pairs. With 20 independent parameters, the RMSE for the static non-linearity model is model is 2.19 for CCC, 1.98 for JKL, and 1.38 for JMF.

To account for contrast induction effects, D'Zmura (1997) proposed a model that has 72 linear color-spatial filters followed by a non-linear contrast normalization process. His model is similar to ours in many respects. The main differences are: (1) In the D'Zmura model the divisive inhibition signal is a linear combination of the linear operator outputs (constants q_j of our model set to 1); (2) In the D'Zmura model, there is a linear dependence of the numerator of the non-linear response function on linear operator output (constants p_j of our model set to 1). Could a model with this form of non-linearity account for our data? Since this model assumes that the exponent to the linear operator excitation is 1, this model lacks the accelerating non-linearity in the response function. The target contrast required to increase the response of one mechanism by a fixed amount is either the same or larger the target absolute threshold. As a result, given the common rule for computing the detection variable (Eq. (8)), it is impossible for a pedestal to facilitate target detection. Thus, this model can only predict masking, but not facilita-

Fig. 5. Fits of different models. Panel (a) is the fit of our chromoluminance pattern detection and masking model. Panel (b) shows the fit of the line element model; panel (c), the rectified linear response model proposed by De Valois and De Valois (1993) (here the functions for the luminance pedestal and the green-red pedestal are the same); panel (d), the power law model with $P < 1$; panel (e), the static non-linearity model and panel (f), the model based on D'Zmura's model.

tion. For a specific stimulus set such as the one we used, D'Zmura's model can implemented as a special case of our model. We created a model similar to D'Zmura's by constraining both the excitatory exponents p_j and inhibitory exponents q_j to 1. Fig. 5(f) illustrates the resulting fit. The model fails dramatically to predict the observed facilitation in these conditions. With 23 free parameters, the RMSE of the fit of this D'Zmura type model is 2.78 for CCC, 2.45 for JKL, and 2.41 for JMF. This model can be viewed as a subset of our model for observers CCC and JKL, so we can perform a statistical test on the goodness-of-fits that takes the difference in the number of parameters into account. The D'Zmura type model fits are statistically worse than our model ($F(6,28) = 10.1533$, $P < 1E-04$ for CCC; $F(6,28) = 7.4574$, $P < 1E-04$ for JKL).

3.2. Comparison of model implications with other results

As described above, our model accounts for our results on chromoluminance pedestal effects. Although we have not fitted the model to other data, it is clear that it can account for most of the effects found in chromoluminance masking literature using sinewave or Gabor targets and pedestals. The most common result is a dipper-shaped TvC function. TvC functions vary greatly in the magnitude of facilitation and the pedestal contrast at which it is maximum. They also vary in the magnitude of masking. The model accounts for these varying forms by different magnitudes of excitation and divisive inhibition. The model accounts for the very broad chromoluminance tuning of masking, which has been widely reported and for the most frequently reported cross-pedestal effects (no facilitation of luminance target detection by isoluminant pedestal and facilitation of detection of isoluminant target detection by luminance pedestal at high pedestal contrast). The model does not make predictions about the spatial tuning of either facilitation or masking. However, since it requires that this tuning depend on both the excitatory and the divisive inhibitory sensitivities of the mechanisms, it has the potential to account for a variety of effects.

3.3. Phase effects

The relative phase between the target and the pedestal has an effect on target threshold (De Valois and Switkes, 1983; Switkes et al., 1988; Chen et al., 1999b). There have been several studies of phase effects in luminance pattern masking. These are reviewed by Foley and Chen (1999) who show that most of these effects can be accounted for by a version of the model that has mechanisms tuned to relative phases of 0, 90, 180, and 270°. The model described in this paper has mechanisms tuned to phases of 0 and 180°, but not 90 and 270°, so it accounts for some phase effects, but not all. However, it could be readily expanded to account for effects at other relative phases. The phase model also assumes changes in detection strategy to account for some of the effects. We deliberately did not include the 90 and 270° mechanisms or the detection strategy variation in this version of the model, because we did not need them to account for our chromoluminance pedestal effects. However, we can describe the predictions that the more complete model makes for phase effects.

The model assumes that mechanism excitation is phase dependent and becomes negative for an out-of-phase pedestal; divisive inhibition, on the other hand is always positive and equal for opposite phase mechanisms. This implies that in cases where the pedestal does not excite the detecting mechanism, as when the pedestal direction is orthogonal to the detecting mechanism direction, there will be masking but not facilitation, and there will be no effect of a change in pedestal phase from 0 to 180°. In a cross-pedestal paradigm, Switkes et al. (1988) (Figs. 9b and 10c) found this result. When the pedestal direction is not orthogonal to the mechanism direction, the effects are more complex. If the effects of the target and the pedestal on the detecting mechanism are in-phase, the TvC function will have the common dipper shape. If they are out-of-phase, the TvC function will rise at low pedestal contrasts, then drop sharply to below the in-phase function, then rise parallel to the in-phase function. The reason for the initial rise is the negative excitation produced by the out-of-phase pedestal. The reason for the sharp drop is that at a certain pedestal contrast it becomes possible to detect the target by a decrement in the response of the out-of-phase mechanism. The reason that the out-of-phase pedestal produces lower thresholds in this range is that the response of the mechanism changes more rapidly on the decrement side than the increment side. Switkes et al. (1988) (Figs. 7, 9a, and 10b) measured the effect of varying the phase of a luminance mask (0 or 180°) relative to an isoluminant red-green grating. They found small phase effects in some conditions. These effects are consistent with our model. At 2 c/deg they found that at low pedestal contrasts the out-of-phase pedestal (green aligned with bright) masked more (Fig. 7, observer: AB). At 0.5 c/deg they found that at high pedestal contrast the in-phase pedestal masked more than the out-of-phase pedestal (Fig. 10b). When they fixed the pedestal at 50 times threshold (Fig. 9a), they found that the in-phase pedestal masked more at spatial frequencies from 0.25 to 4 c/deg. These effects are small and one could argue whether some of them are real, but the main point is that there is more consistency than inconsistency with

our model's predictions here. It is interesting that the green/red mechanism required to account for these results within the context of our model has a stronger M- than L-cone input, consistent with what is required to account for our measurements. De Valois and Switkes (1983) (Figs. 5 and 6) also measured cross-pedestal effects with the pedestal at 90° phase relative to the target as well as 0 and 180°. The model of Foley and Chen (1999) predicts that a pedestal at 90° will mask more than one at 0 or 180° when all four phase mechanisms are used to detect. De Valois and Switkes did not find a consistent effect of phase in either crossed condition, although in two of the four cases masking was greatest at 90°.

3.4. Noise masking

In the preceding paper we gave a brief description of chromoluminance masking with noise masks and pointed out the differences between pattern masking and noise masking both in the phenomena and the models used to account for them. The principal differences are the absence or small magnitude of facilitation in noise masking and the absence of cross-masking. We have not either predicted or explained these effects, although it may be possible to account for them with an expanded version of our model. A first step would be an analysis of the spatio-temporal spectra of these stimuli and a comparison of this with the excitatory and divisive inhibitory sensitivities of the mechanisms on the relevant dimensions. However, since these stimuli and their representation in the visual system are much more complex than simple patterns, it is likely that there will be differences in detection strategy as well (see Ahumada & Beard, 1997).

3.5. Spectral sensitivity of pattern detection mechanisms

Although we do not yet have a general model of stimulus context effects (including periodic pattern, spots, and noise) on chromoluminance pattern detection and it appears that such a model will be complex by virtue of the nature of the mechanisms and the large number of mechanisms with different spatio-temporal sensitivities that are involved, there are some encouraging points of agreement about the spectral sensitivity of these mechanisms. Most theorists agree that the mechanisms involved in pattern detection have three types of spectral sensitivity functions: one (LUM) sums the three cone outputs; a second (RG) differentiates L- and M-cone outputs; and the third (BY) may differentiate L and $M+S$ or $L+M$ and S. These mechanisms are thought to combine cone excitations linearly. This literature is reviewed by Eskew, McLellan and Giulianini (in press).

Our mechanism spectral sensitivities are consistent with this general picture. There is, however, one notable difference between the relative contrast weights that we found and those found by others. Studies of detection (Sankeralli & Mullen, 1996) and noise masking (Sankeralli & Mullen, 1997; Giulianini & Eskew, 1998) have concluded that the GR and RG mechanisms weight the L- and M-cone contrasts about equally, at least for most observers. For each of our three observers the M weight is greater than the L weight. This is critical to the model's ability to account for the facilitation produced in the isoluminant target, luminance pedestal condition. There are a number of ways to explain the difference. (1) There could be considerable inter-observer variability in the spectral sensitivity of RG. (2) The spectral sensitivity of RG could vary with the spatio-temporal properties of the detecting mechanism. Our stimuli were of shorter duration than those used in the other studies. (3) As suggested by Switkes et al. (1988), the substrate of the RG pathway may be a collection of cells with a range of spectral sensitivities. In this case, we can imagine that different cells mediate performance under different experimental conditions. (4) Our model's account of facilitation could be too simple. There is evidence that for some stimulus conditions there is a facilitatory process that does not involve excitation of the detecting mechanism by the pedestal (Cole et al., 1990). Although it might be possible to extend the model in any of these directions, the model in its present form provides a parsimonious account for our data.

We have presented a model of chromoluminance pattern detection. The model draws its general structure both from the pattern vision and color vision literatures. The fact that the model provides a good account of a large set of detection and discrimination data for chromoluminance patterns is encouraging: it suggests that ideas that have come from research with luminance patterns and ideas from research with chromoluminance spots can be combined to account for pattern pedestal effects with chromoluminance patterns.

The model we present is somewhat complex in that it postulates multiple mechanisms, non-linear mechanism responses, and broadly tuned divisive inhibition. We have provided evidence, however, that each of these features is required by the data by showing that models that lack one of them do not describe it well. It is not just that the simplified versions of the model fit poorly; they also fail to capture major qualitative features of the data. At the same time, we concede that our model does not fit the data perfectly and in some instances the failures are systematic. We have not been able formulate a model that eliminates these weaknesses. Nevertheless, we think that this model is a step toward a more complete understanding of chromoluminance pattern vision.

Acknowledgements

This research was conducted as part of the first author's Ph.D. dissertation project. Preliminary versions were presented at the 1997 ARVO annual meetings and at the 1996 meeting of the Optical Society of America (Chen, Foley, & Brainard, 1997). Supported by NIH EY10016.

References

Ahumada, A. J., & Beard, B. L. (1997). Image discrimination models predict detection in fixed but not random noise. *Journal of the Optical Society of America A*, *14*, 2471–2476.

Albrecht, D. G., & Geisler, W. S. (1991). Motion Sensitivity and the contrast-response function of simple cells in the visual cortex. *Visual Neuroscience*, *7*, 531–546.

Boynton, G. M., & Foley, J. M. (1999). Temporal sensitivity of human luminance pattern mechanisms determined by masking with temporally modulated stimuli. *Vision Research*, *39*, 1641–1656.

Cavanagh, P. (1991). Vision at equiluminance. In J. J. Kulikowski, V. Walsh, & I. J. Murray, *Limits of vision*. Boca Raton: CRC Press.

Chen, C. C., Foley, J. M, & Brainard, D. H. (1997). Detecting chromatic patterns on chromatic pattern pedestals. IS&T/OSA proceedings: Optics & Imaging in the Information Age, 19–24.

Chen, C. C., Foley, J. M, & Brainard, D. H. (2000). Detection of chromoluminance patterns on chromoluminance pedestals I: threshold measurements. *Vision Research 40*, 773–788.

Chen, C. C., Foley, J. M., & Brainard, D. H. (1999). Divisive inhibition model for chromoluminance pattern equidiscrimination contours. *SPIE Proceedings*, *3644*, 78–87.

D'Zmura, M. (1997). Color contrast gain control. In W. Backhaus, R. Kliegle, & J. Werner, *Color vision*. New York: Walter and Gruyter.

DeMarco, P., Pokorny, J., & Smith, V. C. (1992). Full-spectrum cone sensitivity functions for X-chromosome-linked anomalous trichromats. *Journal of the Optical Society of America A*, *9*, 1465–1476.

De Valois, R. L., & De Valois, K. K. (1988). *Spatial vision*. Oxford: Oxford University Press.

De Valois, R. L., & De Valois, K. K. (1993). A multi-stage color model. *Vision Research*, *33*, 1053–1065.

De Valois, K. K., & Switkes, E. (1983). Simultaneous masking interactions between chromatic and luminance gratings. *Journal of the Optical Society of America*, *73*, 11–18.

Eskew, R. T., Jr., McLellan, J. S., & Giulianini, F. Chromaticdetection and discrimination. In K. Gegenfurtner, & L. T. Sharpe, Color vision: from molecular genetics to perception. Cambridge: Cambridge University Press (in press).

Fechner, G. (1859/1966). Elements of psychophysics (translated by Adler, H. E.). New York: Holt.

Foley, J. M. (1994). Human luminance pattern-vision mechanisms: Masking experiments require a new model. *Journal of the Optical Society of America A*, *11*, 1710–1719.

Foley, J. M., & Chen, C. C. (1997). Analysis of the effect of pattern adaptation on pattern pedestral effects: a two-process model. *Vision Research*, *37*, 2779–2788.

Foley, J. M., & Chen, C. C. (1999). Pattern detection in the presence of maskers that differ in spatial phase and temporal offset: threshold measurements and a model. *Vision Research*, *39*, 3855–3876.

Giulianini, F., & Eskew, R. T. Jr. (1998). Chromatic masking in the (ΔL/L, (M/M) plane of cone contrast space reveal only two detection mechanisms. *Vision Research*, *38*, 3913–3926.

Graham, N. (1989). *Visual pattern analyzers*. Oxford: Oxford University press.

Guth, S. L., Massof, R. W., & Benzschawel, T. (1980). Vector model for normal and dichromatic color vision. *Journal of the Optical Society of America*, *70*, 197–212.

Guth, S. L. (1991). Model for color vision and light adaptation. *Journal of the Optical Society of America*, *8*, 976–993.

Heeger, D. J. (1992). Normalization of cell responses in cat striate cortex. *Visual Neuroscience*, *9*, 181–197.

Helmholtz, H. (1896). *Treatise on physiological optics*. New York: Dover.

Hurvich, L. M., & Jameson, D. (1957). An opponent-process theory of color vision. *Psychological Reviews*, *64*, 384–404.

Krauskopf, J., Williams, D. R., Mandler, M. B., & Brown, A. M. (1986). Higher order color mechanisms. *Vision Research*, *26*, 23–31.

Le Grand, Y. (1949). Color difference thresholds in Young's theory. (translated by K. Knoblauch). *Color Research and Application*, *19*, 296–309.

Legge, G. E., & Foley, J. M. (1980). Contrast masking in human vision. *Journal of the Optical Society of America*, *70*, 1458–1470.

Li, A., & Lennie, P. (1997). Mechanisms underlying segmentation of colored textures. *Vision Research*, *37*, 83–98.

Mullen, K. T., & Kingdom, F. A. A. (1991). Colour contrast in form perception. In P. Gouras, *The perception of colour*. Boca Raton: CRC Press.

Poirson, A. B., & Wandell, B. A. (1996). Pattern-color separable pathways predict sensitivity to simple colored patterns. *Vision Research*, *36*, 515–526.

Press, W. H., Teukolsky, S. A., Vetterling, W. T., & Flannery, B. P. (1986). *Numerical recipes*. Cambridge: Cambridge University Press.

Quick, R. F. (1974). A vector-magnitude model of contrast detection. *Kybernetik*, *16*, 65–67.

Regan, D. (1991). Spatial vision for objects defined by colour contrast, binocluar disparity and motion parallax. In D. Regan, *Spatial vision*. Boca Raton: CRC Press.

Ross, J., & Speed, H. D. (1991). Contrast adaptation and contrast masking in human vision. *Proceedings of the Royal Society London Series B*, *246*, 61–69.

Sankeralli, M. J., & Mullen, K. T. (1996). Estimation of the L-, M-, and S-cone weights of the postreceptoral detection mechanisms. *Journal of the Optical Society of America A*, *13*, 906–915.

Sankeralli, M. J., & Mullen, K. T. (1997). Postreceptoral chromatic detection mechanisms revealed by noise masking in three dimensional cone contrast space. *Journal of the Optical Society of America A*, *14*, 2633–2646.

Sekiguchi, N., Williams, D. R., & Brainard, D. H. (1993). Aberration-free measurements of the visibility of isoluminant gratings. *Journal of the Optical Society of America A*, *10*, 2105–2117.

Smith, V. C., & Pokorny, J. (1975). Spectral sensitivity of the foveal cone photopigments between 400 and 500 nm. *Vision Research*, *15*, 161–171.

Switkes, E., Bradley, A., & De Valois, K. K. (1988). Contrast dependence and mechanisms of masking interactions among achromatic and luminance gratings. *Journal of the Optical Society of America A*, *2*, 62–71.

Teo, P. C., & Heeger, D. J. (1994). Perceptual image distortion. *SPIE Proceedings*, *2179*, 127–141.

Vos, J. J. (1978). Colorimetric and photometric properties of a 2° fundamental observer. *Color Research and Application*, *3*, 125–128.

Wandell, A. B. (1982). Measurement of small color difference. *Psychological Review*, *89*, 281–302.

Watson, A. B., & Solomon, J. A. (1997). Model of visual contrast gain control and pattern masking. *Journal of the Optical Society of America A*, *14*, 2379–2391.

Webster, M. A., & Mollon, J. D. (1991). Changes in colour appearance following post receptoral adaptation. *Nature*, *349*, 235–238.

Wilson, H. R., Levi, D., Maffei, L., Rovamo, J., & De Valois, R. (1990). The perception of form: retina to striate cortex. In L. Spillmann, & J. S. Werner, *Visual perception: the neurophysiological foundations* (pp. 231–272).

Wilson, H. R., McFarlane, D. K., & Philips, G. C. (1983). Spatial frequency tuning of orientation selectivity units estimated by oblique masking. *Vision Research*, *23*, 873–882.

Wyszecki, G., & Stiles, W. S. (1982). *Color science: concepts and methods*, *quantitative data and formulae* (2nd ed.). NY: Wiley.